

An Effective Investigation On Synthesis And Opto-Electronic Properties of Er³⁺ Doped Tellurite Based Glasses

Mayank Bhargav¹, Dr. Vijetha Yadav², Dr. Vamshi Talla³

¹Research Scholar, Madhyanchal Professional University (MPU), Department of ECE Bhopal, India

²Supervisor, Madhyanchal Professional University (MPU), Department of ECE

³Co-Supervisor, Department of ECE, Talla Padmavati College of Engineering, Tekulagudem (Somidi), Kazipet, Warangal-Telangana, (India),

Corresponding Author: Mayank Bhargav

Abstract –This paper presents a comprehensive investigation of two strategically significant domains in modern photonics and optical communication systems: (i) the development and characterization of Er³⁺-Yb³⁺ codoped bismuth-tellurite glasses for efficient frequency up conversion, and (ii) the performance enhancement of erbium-doped fiber amplifiers (EDFAs) through an intelligent Adaptive Multi-Stage EDFA Optimization (AMEDO) algorithm. By addressing both material-level and system-level challenges, this work contributes to the advancement of next-generation optical technologies. In the first part, Er³⁺-Yb³⁺ codoped bismuth-tellurite glasses were synthesized via the melt-quench technique. Structural and thermal analyses confirmed their amorphous nature, good thermal stability, and favorable glass-forming ability. Systematic variation of erbium concentration revealed significant modifications in physical and structural parameters, indicating the formation of non-bridging oxygen's and network restructuring. Optical absorption studies verified efficient sensitizer-activator coupling, with strong Yb³⁺ absorption near 980 nm. Under 980 nm excitation, intense green and red up conversion emissions were observed, governed by energy transfer and excited-state absorption mechanisms. An optimal Er₂O₃ concentration of approximately 0.5 mol% was identified to achieve maximum emission intensity before concentration quenching effects dominated. The high refractive index and controlled structural disorder of the prepared glasses demonstrate their suitability for solid-state lasers, displays, sensors, and bio photonic applications

Keywords: Bismuth Tellurite Glasses, Er³⁺/Yb³⁺ Co-doping, Optical Up conversion, Rare Earth Ions, Tellurite Glass Matrix, Photonic Materials, Luminescence Properties, Green Emission, Red Emission, Energy Transfer Mechanism, Excited State Absorption (ESA), Up conversion Luminescence, 980 nm Excitation.

I. INTRODUCTION

Lanthanide ions are well known for their ability to convert electromagnetic frequencies from low to high or vice versa through a multi-phonon absorption process. The conversion of incident low-frequency radiation into higher-frequency radiation is referred to as optical up conversion (UC). This unique phenomenon has drawn significant research attention due to its applications in the field of optoelectronics. Tellurite oxide (TeO₂) based glasses codoped with lanthanide ions exhibit remarkable features and are widely used in optoelectronic devices. Compared with borate and silicate glasses, Tellurite-based glasses offer superior lanthanide solubility, higher thermo-mechanical durability and a lower cutoff wavelength. Lanthanide ions are used in frequency up conversion processes for applications in lasers, optical fibers, biosensors, thermal sensors, solar cells and other luminescent and photonic devices. These glasses attract researchers because of their high luminescence intensity which makes them suitable for display technologies. The up conversion process is based on Raman's anti-Stokes phenomenon, in which lanthanide ions absorb two or more photons of higher wavelength and emit radiation of shorter wavelength. Trivalent lanthanide ions such as Tm³⁺, Ho³⁺, Er³⁺, Eu³⁺, Nd³⁺ and Yb³⁺ are commonly used to enhance up conversion emission in the visible to infrared region. In diagnostic applications, frequency up conversion plays an important role. Among lanthanides, Erbium (Er³⁺) ions are particularly interesting because of their multiple energy states within the glassy lattice. When combined with Ytterbium (Yb³⁺) ions, the up conversion efficiency is further enhanced. Yb³⁺ ions exhibit strong absorption near 980 nm and efficiently transfer this energy to Er³⁺ ions [8], resulting in visible green emission around 530 nm (²H_{11/2}→⁴I_{15/2}) and 550 nm (⁴S_{3/2}→⁴I_{15/2}) upon 980 nm excitation. For practical applications, the choice of the glass former and batch composition is crucial. Among various glasses, Tellurite glass is highly desirable due to its broad transmission window, low melting

temperature, high refractive index, low optical losses and excellent thermal and chemical durability. In this paper, the physical, thermal, optical, and frequency up conversion properties of bismuth-tellurite glasses codoped with Er^{3+} - Yb^{3+} ions are reported and analyzed.

II. EXPERIMENTAL DETAILS

Preparation of Glass Samples

A series of Bismuth-Tellurite glasses codoped with Er_2O_3 - Yb_2O_3 were synthesized by the melt-quench method. The glass compositions were formulated as:

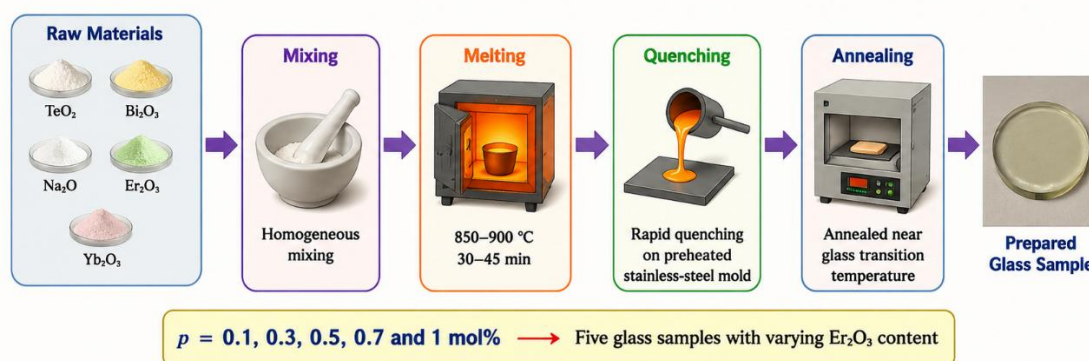
(79.5-p)% TeO_2 -10% Bi_2O_3 -10% Na_2O -p% Er_2O_3 -0.5% Yb_2O_3 where $p = 0.1, 0.3, 0.5, 0.7$ and 1 mol%

Preparation of Glass Samples

A series of Bismuth-Tellurite glasses codoped with Er_2O_3 - Yb_2O_3 were synthesized by the melt-quench method. The glass compositions were formulated as:

(79.5-p)% TeO_2 -10% Bi_2O_3 -10% Na_2O -p% Er_2O_3 -0.5% Yb_2O_3

where $p = 0.1, 0.3, 0.5, 0.7$ and 1 mol%.



The samples were labeled as BTEY1, BTEY2, BTEY3, BTEY4 and BTEY5.

High purity chemicals were weighed accurately (~15 g batches) using a digital balance. The powders were mixed thoroughly in an agate mortar and melted in an alumina crucible at 900°C, followed by heating at 950°C for 30 minutes. The homogeneous melt was poured into preheated molds and then annealed at 300°C for 2 hours to remove thermal stress.

III. CHARACTERIZATION TECHNIQUES

- (i) Differential Scanning Calorimetric (DSC): To determine the glass transition, melting and crystallization temperatures.
- (ii) X-Ray Diffraction (XRD): To verify the amorphous nature of the samples.
- (iii) UV-VIS-IR Absorption Spectroscopy: To determine absorption peaks and optical band gaps.
- (iv) Photoluminescence (PL) Spectroscopy: To study the frequency up conversion behaviour under 980 nm excitation.
- (v) Physical parameters such as density, molar volume, lanthanide ion concentration, polaron radius, inter-ionic distance and field strength were calculated using standard relations.

IV. RESULTS AND DISCUSSION

4.1 Thermal Analysis

For the thermal characterization differential scanning calorimetry (DSC) of the BTEY1 have been done by TA Instruments, USA; Q 10. In the temperature range 40.00°C to 490.00°C at 10°C/Minute heating rate. The plot of temperature and heat flow is shown in the figure1. Thermal characteristic temperatures as transition temperature (T_g), melting temperature (T_m) and crystallization temperature (T_c) of BTEY1 sample observed respectively 310 °C, 350°C and 460°C respectively.

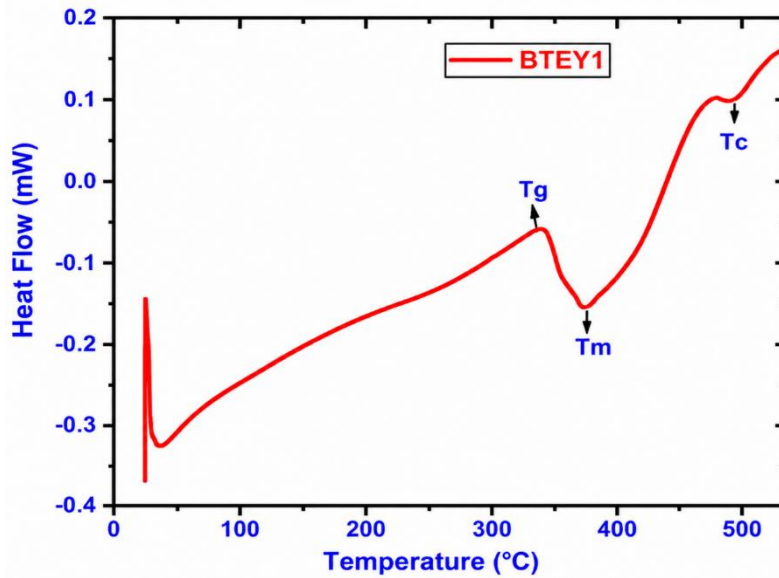


Figure 1 DSC plot of BTEY1 sample

The DSC curve of BTEY1 (Figure 1) shows characteristic temperatures: Glass transition temperature (T_g): 310°C Melting temperature (T_m): 350°C Crystallization temperature (T_c): 460°C These values confirm the thermal stability of the synthesized glass.

4.1.1X-Ray Diffractogram

For the authentication of glassiness of the sample (BTEY1) x-ray diffractogram is studied. This characterization is done by Bruker Model No. D2 Phaser 2nd Gen. The angle 2theta is chosen 0° to 70°. Two wide protuberances near 10° and 30° were noticed, no sharp peak confirm amorphous nature of the sample (figure 2).

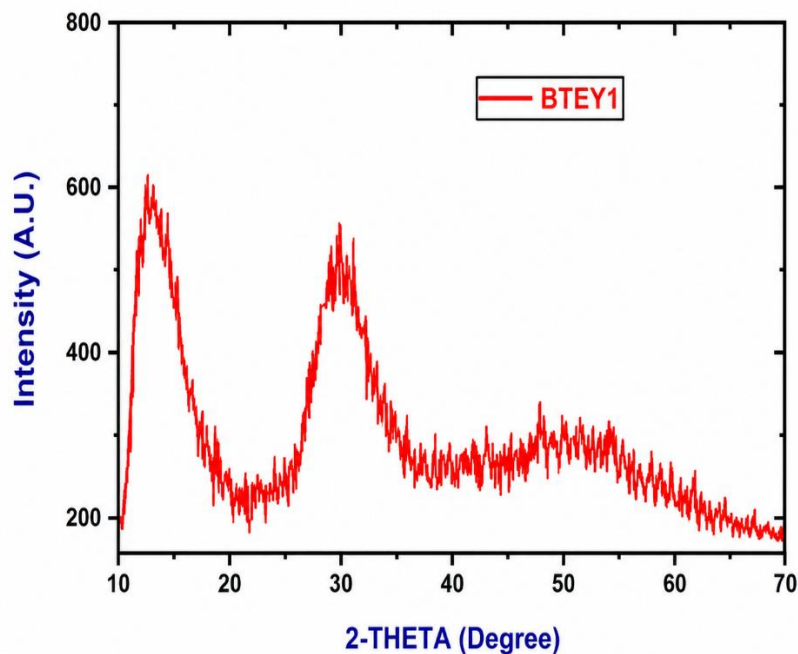


Figure 2. X-Ray diffractogram of BTEY1 sample.

Figure 2. X-Ray diffractogram of BTEY1 sample.

4.1.2 Physical Properties

4.1.2.1 Density

The density (d) is basic physical quantity of any solid sample which can be measured. Measurement of density can be done by using Archimedes principle. Distilled water of density dw is used as immersion liquid

$$d = \frac{\omega_1}{\omega_1 - \omega_2} dw \quad (1)$$

137

► Where, ω_1 and ω_2 are the weights of the synthesized samples in air and in distilled water.

4.3.3.2 Molar Volume

The molar volume (Vm) were calculated by the g relation

$$V_m = \frac{M}{d} \quad (2)$$

Here, M is the molar mass of synthesized samples.



Variation density and molar volume with concentration of lanthanide Erbium ions is shown in figure3. With rising of erbium ions concentration, density of synthesized samples rises whereas molar volume decreases.

4.3.3.3 Lanthanide Ion Concentration

Lanthanide ions concentration (C_L) (ion/cm³) in glass samples can be evaluated by using equation [21]:

$$C_L = C \times N \quad (3)$$

- N is Avogadro number and
- C is lanthanide ions concentration in mole per liter and given as

$$C = \left(\frac{m \times d}{m \times M_w} \right) a \quad (4)$$

- Where 'm' is the mass of lanthanide oxide in gm,
- m is the total mass of the batch in gm,
- M_w is the molecular mass of lanthanide oxide and
- a = 2 (one mole of lanthanide oxide having 2 moles of Er³⁺ ions).

4.3.3.2 Molar Volume

The molar volume (Vm) were calculated by the g relation

$$V_m = \frac{M}{d} \quad (2)$$

Here, M is the molar mass of synthesized samples.

Variation density and molar volume with concentration of lanthanide Erbium ions is shown in figure3. With rising of erbium ions concentration, density of synthesized samples rises whereas molar volume decreases.

4.1.2.2 Lanthanide Ion Concentration

Lanthanide ions concentration (C_L)(ion/cm³) in glass samples can be evaluated by using equation [21]:

$$C_L = C \times N \quad (3)$$

N is Avogadro number and C is lanthanide ions concentration in mole per liter and given as

$$C = \left(\frac{m' \times d}{m \times M_w} \right) a \quad (4)$$

Where „ m' “ is the mass of lanthanide oxide in gm, m is the total mass of the batch in gm, M_w is the molecular mass of lanthanide oxide and $a = 2$ (one mole of lanthanide oxide having 2 moles of Er^{3+} ions).

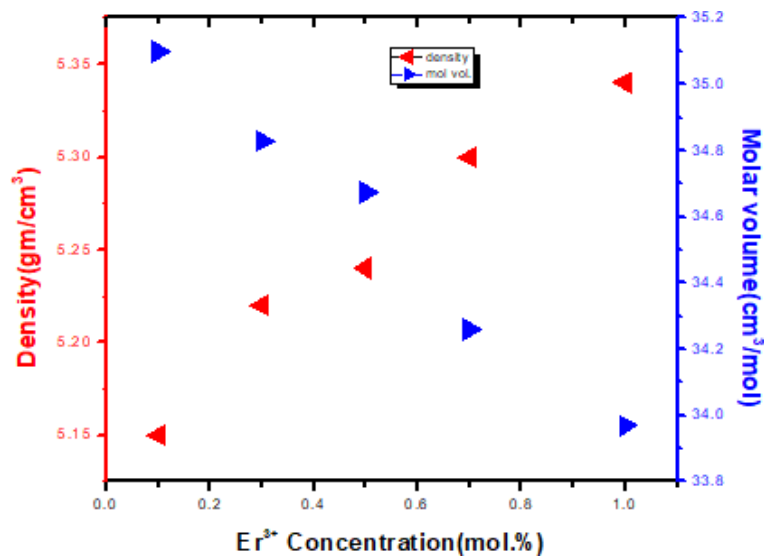


Figure .3. Variation heaviness and molar volume with concentration of Erbium ions

4.1.2.3 Polaron radius (R_p), Inter Ionic Distance (R_i) and Field Strength (F_L)

To the polaron radius help to get information of electron-atom interaction in the solid, it is calculated by using relation [5]

$$R_p = \left(\frac{\pi}{6} C_L \right)^{1/3} \quad (5)$$

The distance between two lanthanide ions calculated by relation

$$R_i = (1 / C_L)^{1/3} \quad (6)$$

For oxidation number of lanthanide ions (X_o) field strength is given as

$$F_L = X_o / R^{1/2} \quad (7)$$

The calculated values of various physical parameters as density (d), Molar volume (V_m), lanthanide ion concentration (C_L), polaron radius (R_p), inter ionic distance (R_i) and Field strength (F_L) are given in table 1.

4.1.2.4 Oxygen Packing Density (OPD)

Further oxygen packing densities of synthesized bismuth tellurite glasses codoped with lanthanide were calculated by using relation

$$OPD = \frac{1000 \times d \times O_x}{M}$$

Where O_x is number of oxygen in the glass sample and M is the molecular mass of the sample. It is observed that with increase of doping of Er_2O_3 oxygen packing density increases, table 1.

Optical Properties

The UV-VIS-IR absorption spectrum of BTEY glasses has been noted in the range of 165 nm to 1250 nm (shown in figure 4). For absorption spectroscopy, spectrometer of Research India model number RI2SA is used. Specific absorption spikes of Er^{3+} ions are observed. These absorption bands are due to transition of electrons from $^4I_{15/2}$ level of Er^{3+} ions to different levels as 377nm ($^4G_{11/2}$), 406nm ($^4H_{9/2}$), 486nm ($^4F_{7/2}$), 520nm ($^2H_{11/2}$), 542nm ($^4S_{3/2}$), 651nm ($^4F_{9/2}$) and 796nm($^4I_{9/2}$). Ytterbium ion perform transition near 980nm correspond to $^2F_{7/2} \rightarrow ^2F_{5/2}$ (figure 4-insat). [4.22-4.25]

Table 1. Physiacal parameters of BTEY glasses

S. No.	Physical Properties	BTEY1	BTEY2	BTEY3	BTEY4	BTEY5
1	Density (d) (g/cm ³)	5.15	5.22	5.24	5.3	5.34
2	Mol. volume(cm ³ /mol)	35.153	34.992	34.943	34.632	34.497
3	Lanthanide ion concentration(c_L) ($c \times 10^{20}$ ions/cm ³)	0.342	1.034	1.723	2.440	3.497
4	Polaron radius (R_p)(Å)	8.601	5.951	5.020	4.470	3.965
5	Inter ionic distance (I_i)(Å)	30.787	21.301	17.968	16.002	14.193
6	Field strength ($F_L \times 10^{13}$) (cm ²)	3.165	6.611	9.295	11.715	14.892
7	Oxygen Packing Density (OPD) (g-atom/l)	57.064	57.384	57.523	58.096	58.410

The direct and indirect allowed energy gaps are very important quantities which are required to study photo electronic transitional structure in both amorphous and crystalline solids. The relation for the forbidden energy gap as function of energy hv at frequency ν is given by expression $\alpha hv = A(h\nu - E_{op})^r$ (9)

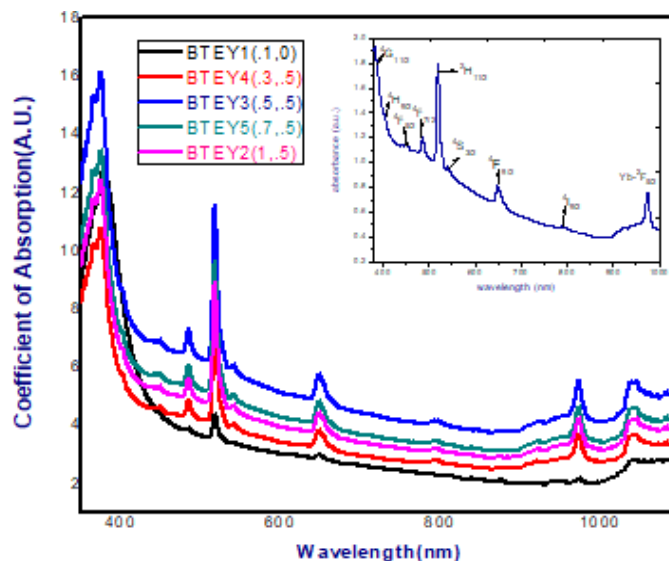


Figure .4. Absorption spectra of BTEY glasses. (inset energy transition in probable levels)

(i)Forbidden Energy Gaps (Eop)

where α is coefficient of absorption, A is constant and r is index. The value of Eop is function of index r. For direct allowed forbidden energy gap index $r = 1/2$ [4.26]. The values of forbidden energy gaps can be calculated by plotting Tauc's graph in the VU region of absorption edge. The Tauc's graph is plotted between $(\alpha hv)^2$ and photon energy hv, the value of direct allowed energy gap (Eop) is the value of hv where

it intersects the linear portion of the curve i.e. $(\alpha h\nu)^2=0$. Figure. 5 is the Tauc's plot for direct allowed energy gap(E_{op}).

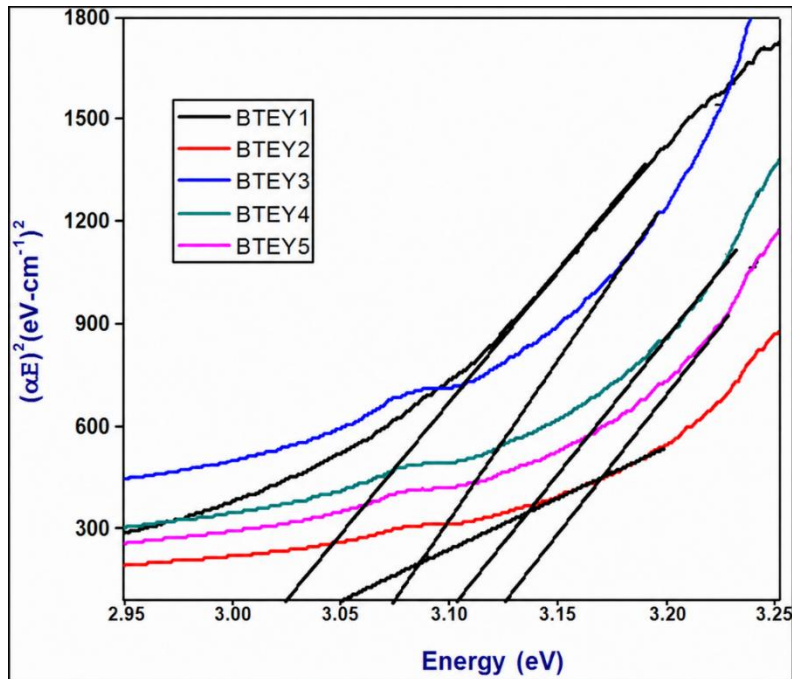


Figure .5 The Tauc's plot for direct allowed energy gap (E_{op})

The value of direct forbidden energy gap of BTEY glasses are lies between 3.02eV to 3.125eV, (Table2).

(ii) Refractive Index (RI)

The relation for RI(n) in terms of forbidden energy gap (E_{op}) is given as [4.27]

$$(n^2 - 1)/(n^2 + 1) = 1 - \sqrt{(E_{op} / 20)} \quad (10)$$

Calculated values of RI of BTEY glasses are given table 2. RI of synthesized glasses is quite high and more than 2.

(iii) Urbatch's Energy (E_u)

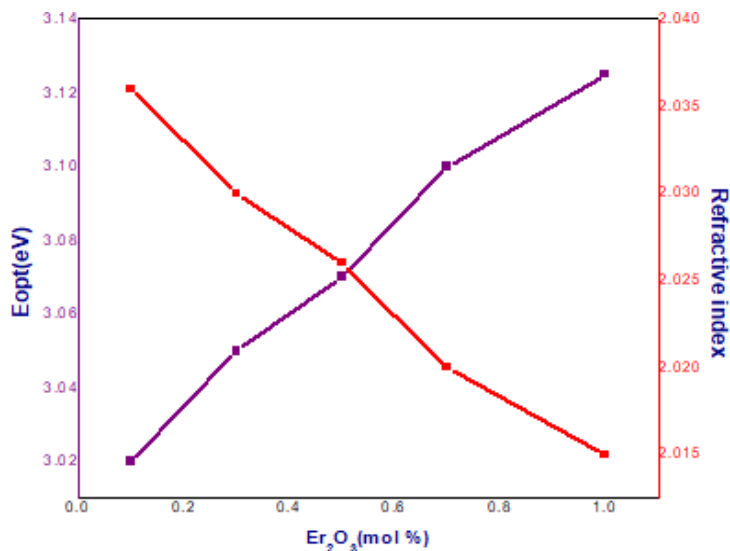


Figure 6 Plot of Energy Band gap & Refractive index with Er_2O_3 concentration.

The Urbach's energy or Urbach's tail (E_u) is a measure of irregular arrangement of elements in the matrix and it is calculated by using Urbach equation [4.28]

$$\ln \alpha = h\nu / E_u + \text{const.} \quad (11)$$

The value of E_u can be estimated from Urbach's plot, i.e. plot of $\ln \alpha$ with respect to photon energy ($h\nu$). E_u is the measure of the reciprocal of slope of linear segment

of the Urbach's plot as shown in figure 6. The values of E_u for BTEY glasses are in the range of 0.25 eV to 0.40 eV, listed in table 2.

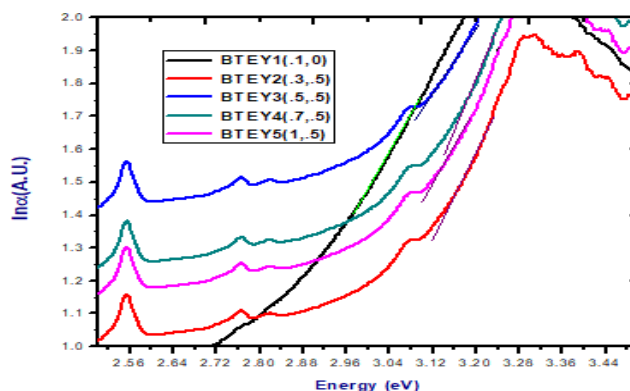


Figure .7 Urbach's plot for BTEY glasses.

Table .2 Optical parameters

S. No.	Physical Properties	BTEY1	BTEY2	BTEY3	BTEY4	BTEY5
1	Cutoff wavelength (nm)	372	370	370	370	371
2	Direct forbidden energy gap (E_{op}) (eV)	3.02	3.05	3.07	3.10	3.125
3	Refractiveindex (RI)	2.036	2.030	2.026	2.020	2.015
4	Urbach's Energy E_u (eV)	0.267	0.250	0.350	0.400	0.320

4.2 Frequency Upconversion Studies

The bismuth tellurite glasses co doped with lanthanide ions as Er^{3+} - Yb^{3+} exhibit excellent frequency up conversion. For the frequency up conversion study of BTEY glasses "Fluorolog -3 of Horriba, Jobin Vyon" PL meter is used with 450-Watt Xenon lamps at excitation of 980nm. Frequency up conversion spectra of BTEY glasses are shown in figure 7. Prominent frequency up conversion is appeared at 524nm, 550nm and at 660nm (Shown in inset figure 7).

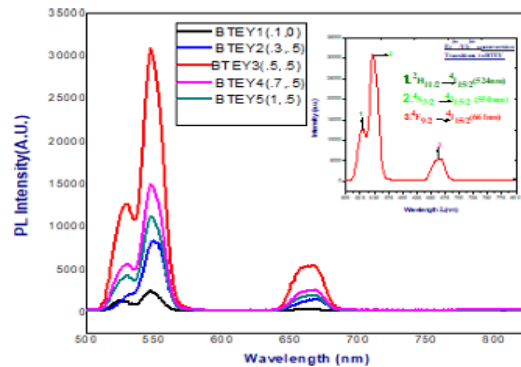


Fig. 7 shows variation of luminescence intensities without changing the position of the peaks with change in the lanthanide ions concentration. As concentration of Er_2O_3 increases from 0.1 to 0.5 mol% emissions increased and on further increasing the concentration of Er_2O_3 from 0.7% to 1%, emission intensity decreases. This variation of emission intensity is due to concentration quenching. In the phenomenon of quenching with increase of erbium ions concentration, energy gets transferred in erbium ions itself and so emission intensity decreases.

Process of energy transfer by 980 nm excitation in Bismuth Tellurite glasses codoped with Er^{3+}/Yb^{3+} , shown in figure 8. Ytterbium and Erbium ions get directly excited by 980 nm excitation energy from level $^2F_{7/2}$ to $^2F_{5/2}$ (Ytterbium ion) and $^4I_{15/2}$ to $^4I_{11/2}$ (Erbium ion). By energy transfer (ET) and excited state absorption (ESA) Er^{3+} ions further excited to $^4F_{7/2}$ and $^4F_{9/2}$ levels subsequently by non-radiative transition populated to $^2H_{11/2}$, $^4S_{3/2}$ and $^4F_{9/2}$. From $^2H_{11/2}$, $^4S_{3/2}$ and $^4F_{9/2}$ levels Erbium ions relax their energy to $^4I_{15/2}$ level and perform green and red upconversion.

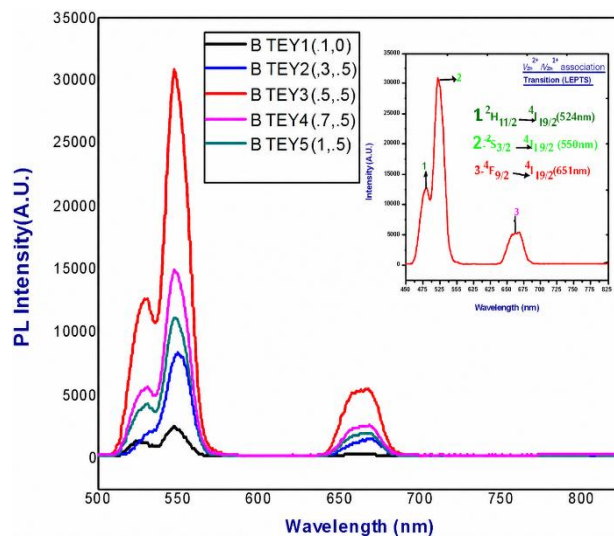


Figure .8 Upconversion Plot for BTEY glasses. (Inset-possible upconversion transitions).

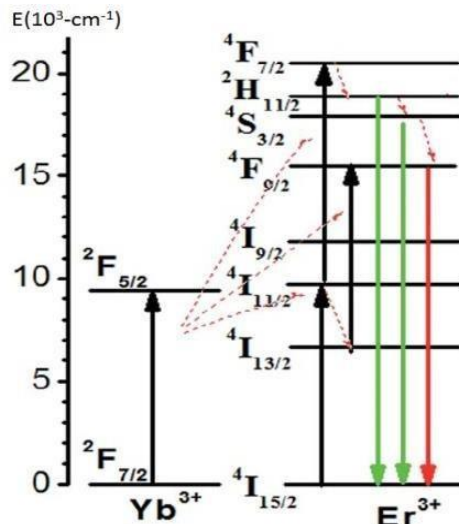


Figure .9 Process of energy transfer by 980nm excitation in bismuth tellurite glasses codoped with Er^{3+}/Yb^{3+}

V.CONCLUSION

Tellurite base glasses doped with bismuth oxide and codoped (Er^{3+} - Yb^{3+}) with different concentrations of erbium were successfully synthesized by classical melting and quenching method. DSC plot reported low temperature melting of tellurite base glass, and X-ray diffractogram confirms its amorphous nature. The role of Er^{3+} ions with various physical characteristics such as Molar volume (V_m), lanthanide ion concentration (c_L), polaron radius (R_p), inter ionic distance (R_i), Field strength (F_L) and oxygen packing density of synthesis glasses are calculated. Interionic distances and average erbium-erbium ion separation were measured and this result confirms of the role on Er^{3+} on structural changes in the glass. The stability of glass structure was studied; it is due to formation of non-bridging oxygen atoms. Optical studies confirm the changes in the Refractive Index (n) of synthesized glasses with the changes in concentration of erbium ions.

The green and red upconversion at 980nm excitation in BTEY glasses codoped with Er^{3+}/Yb^{3+} is due to transition from level $2F_{7/2}$ to $2F_{5/2}$ (Ytterbium ion) and $4I_{15/2}$ to $4I_{11/2}$ (Erbium ion). By energy transfer (ET) and exited state absorption (ESA) Er^{3+} ions further excited to $4F_{7/2}$ and $4F_{9/2}$ levels subsequently by nonradiative

REFERENCES

- [1]. Hemlata Kumari, Ghizal F Ansari, SK Mahajan, K Sk Rezaul, Sukhdev Bairagi, "Study of visible upconversion luminescence in Er^{3+} and Er^{3+}/Yb^{3+} doped tungsten tellurite glasses" Materials Today: Proceedings 59 (2022) 1127-1131, doi.org/10.1016/j.matpr.2022.03.027.
- [2]. Ghizal F Ansari, Sachin Kumar Mahajan, J Parashar, "Intense Upconversion Luminescence of Yb^{3+} - Er^{3+} in Li2O Content Tungsten-tellurite Glasses" J Fluoresc (2011) 21:1337-1342, DOI 10.1007/s10895-011-0864-9
- [3]. Agrawal G.P., Fiber optic communication systems, John Wiley & Sons, New York, 1997.
- [4]. Giles C.R., Desurvire E., "Modelling Erbium-Doped Fiber Amplifiers", Journal of Lightwave Technology Letters, Vol. 9, No 2, 271-283, 1991.
- [5]. Desurvire E., "Erbium doped fiber amplifiers: principles and applications", John Wiley & Sons, New York, 1994.
- [6]. Altuncu A., Siddiqui A.S., Ellis A., Newhouse M.A., Antos A.J. " Gain and noise figure characterization of a 68 km long distributed erbium doped fibre amplifier ", Electronics Letters, Vol.32, No.19, 1800-1801, 1996.
- [7]. A.Cem ÇOKRAK. Ahmet ALTUNCU., "Gain and noise figure performance of Erbium doped fiber amplifier. (EDFA)", JOURNAL OF ELECTRICAL & ELECTRONICS ENGINEERING, 2004.
- [8]. Vasudevan, B, Sivasubramanian, A & Ramesh Babu, M.,,Analysis on Nonlinear characteristics of EDFA in single channel dispersion compensated and uncompensated Telecommunication System", International Journal of Applied Engineering Research ISSN 0973-4562, vol. 10, no. 23, pp. 43318-43327(Annexure-II), 2015.
- [9]. Vasudevan, B, Sivasubramanian, A & Ramesh Babu, M.,,Optical Study on Er-Yb Co-doped Borotelluite Glasses for Optical Amplifiers", Journal of Optoelectronics and Advanced Materials. E-ISSN1841-7132, P-ISSN 1454-4164, vol.19, no. 1-2, pp.11-15 (Annexure-I), 2017.
- [10]. T. Subramaniam, M. A. Mahdi, F. R. Mahamd Adikan, P. Poopalan and H. Ahmad, Gain and noise properties of self-saturated erbium doped fiber amplifiers, TENCON Proceedings. Intelligent Systems and Technologies for the New Millennium (Cat. No.00CH37119), Kuala Lumpur, Malaysia (2000) pp. 424-426 vol.3.
- [11]. R. Anthony, S. Pain and S. Biswas, Double pass erbium doped fiber amplifier with 100nm broadband optical amplification for CATV transmission system, International Conference on Communications, Devices and Intelligent Systems (CODIS), Kolkata, India (2012) pp. 397-400.

- [12]. J. B. Rosolem, M. R. X. de Barros, A. A. Juriollo and M. R. Horluchi, Double pass L band erbium doped fiber amplifier with an embedded DCF, Proceedings of the 2003 SBMO/IEEE MTT-S International Microwave and Optoelectronics Conference - IMOC 2003. (Cat. No.03TH8678), Foz do Iguacu, Brazil (2003) pp. 121-123 vol.1.
- [13]. A. Shah and P. Mankodi, Analysis and simulation on gain flattening filter of an erbium doped fiber amplifier for multi-channel WDM system, International Conference on Wireless Communications, Signal Processing and Networking (WiSPNET), Chennai, India (2017) pp. 458-462.